# Rate Constants of Nine C6−C9 Alkanes with OH from 230 to 379 K: Chemical Tracers for [OH]

**Michele M. Sprengnether[†] and Kenneth L. Demerjian**

*Atmospheric Sciences Research Center, State University of New York, Albany, New York, 12203*

**Timothy J. Dransfield***

*Department of Chemistry, University of Massachusetts, 100 Morrissey Blvd., Boston, Massachusetts, 02125*

**James S. Clarke[‡] and James G. Anderson**

*Department of Chemistry and Chemical Biology, Harvard University, 12 Oxford Street, Cambridge, Massachusetts, 02138*

**Neil M. Donahue**

*Center for Atmospheric Particle Studies, Doherty Hall B204, Carnegie Mellon University, Pittsburgh, Pennsylvania, 15213*

*Received: November 26, 2008; Revised Manuscript Received: February 18, 2009*

We report absolute rate-constant measurements for the reactions of nine $C_6-C_9$ alkanes with OH in 8−10 torr of nitrogen from 230 to 379 K in the Harvard University High-Pressure Flow System. Hydroxyl concentrations were measured using laser-induced fluorescence, and alkane concentrations were measured using Fourier transform infrared Spectroscopy. Ethane's reactivity was simultaneously measured as a test of experimental performance. Results were fit to a modified Arrhenius equation based on transition state theory (ignoring tunneling), $k(T) = Be^{-E_a/T}/(T(1 - e^{-1.44\nu_1/T})^2(1 - e^{-1.44\nu_2/T})$, with $\nu_1$ and $\nu_2$ bending frequencies, set to 280 and 500 $cm^{-1}$. Results were as follows for $B$ ($10^{-9}$ K $cm^3$ $s^{-1}$), $E_a$ (K), and $k(298)$ ($10^{-12}$ $cm^3$ $s^{-1}$): cyclohexane, 3.24 ± 0.14, 332 ± 12, 7.13; cyclo-octane, 3.47 ± 0.30, 149 ± 26, 14.1; 2-methylhexane, 1.45 ± 0.08, 110 ± 15, 6.72; 3-methylhexane, 1.50 ± 0.08, 128 ± 16, 6.54; methylcyclopentane, 1.65 ± 0.07, 109 ± 13, 7.65; methylcyclohexane, 1.86 ± 0.09, 83 ± 14, 9.43; methylcycloheptane, 3.45 ± 0.45, 142 ± 36, 14.4; *n*-propylcyclohexane, 2.83 ± 0.14, 112 ± 15, 13.0; isopropylcyclohexane, 1.79 ± 0.11, −44 ± 34, 13.9. Uncertainties are one $\sigma$ results from linear regression fits and are likely underestimated. Room temperature rate coefficients of reaction are accurate to within 10% at two $\sigma$. A comprehensive fit to 17 separate studies including the present work for cyclohexane gives good agreement with the present results: terms as above, 3.09 ± 0.12, 326 ± 12, 6.96. Five of these compounds are routinely measured in urban air within a suite of atmospheric nonmethane hydrocarbons and reach parts per billion levels. The remaining four are C8−C9 cycloalkanes with low anthropogenic emissions. Because of their high, specific reactivity with OH, their concentration decays may be used as an indirect measurement of [OH] in the atmosphere or laboratory. This data set serves to further constrain the reaction barriers for cyclohexane and cyclo-octane, is the first temperature-dependent study for methylcyclopentane and methylcyclohexane, and provides the first measurements for the rate constants of the remaining five hydrocarbons. Reactivity follows general trends observed for other saturated alkanes, increasing with size and extent of substitution. Reaction barriers are heavily influenced by the presence of tertiary hydrogens. The reaction barrier for cyclo-octane is significantly lower than that for cyclohexane, a result that is not predicted from our current understanding of hydrocarbon reactivity.

## Introduction

The selective reactivity of aromatic and saturated hydrocarbons with OH has been employed as an indirect measure of OH radical concentration in the laboratory[1−3] as well as the atmosphere.[4−6] This [OH] measurement depends upon accurate knowledge of the rate of reaction and the resulting hydrocarbon depletion. Competing reactions must be insignificant or well-defined. While alkenes offer the highest rates of reaction with OH, they usually exhibit additional reactivity with other atmospheric species, such as ozone. Both saturated hydrocarbons and aromatic compounds have negligible reaction with ozone, so they meet the criterion for selective reactivity with atmospheric OH. A field campaign in which both aromatic and saturated hydrocarbons are utilized for indirect measure of ambient [OH] offers a valuable cross verification that both species did not have competing chemistry or potential local sources.[7] Atmospheric diffusion also affects relative hydrocarbon concentrations and can complicate any indirect measurement of [OH].[8] Recent work using hydrocarbons as indirect probes

* To whom correspondence should be addressed. E-mail: timothy.dransfield@umb.edu. Fax: 617-287-6030. Phone: 617-287-6143.
[†] Present address: 31 Chilton St., Cambridge, Massachusetts 02138.
[‡] Present address: Intel Corporation, RA3-252, 2501 NW 229th Ave., Hillsboro, Oregon, 97124.

10.1021/jp810412m CCC: $40.75 
Published on Web 03/31/2009

of atmospheric [OH] has focused on examining species with varying lifetimes relative to OH reaction and examining their spatial and temporal variability[9−11] or looking at their relative decay within a specific air flow.[12−17]

The $C_6-C_7$ alkanes in this kinetics study (cyclohexane, methylcyclopentane, methylcyclohexane, 2-methylhexane, and 3-methylhexane) reach hundreds of pptv−ppbv levels in urban air and have an atmospheric lifetime with respect to OH of a few days. This makes them potential candidates for the indirect determination of [OH] within an urban plume. Only one atmospheric study to date has used any of these species in such a manner. 2-methylhexane was used by Kramp.[13] A study in England[6] measured cyclohexane, and levels were too low in the downwind urban plume to infer [OH]. Toluene was used to measure indirect [OH] in a Sacramento California urban plume.[15]

Broader use of these tracers is possible. On the basis of the median relative concentrations of the most abundant hydrocarbons in 39 U.S. cities summarized by Seila,[18] three of the species, 2- and 3-methylhexane and methylcyclopentane, have urban concentrations nearly a factor of 5 below toluene and roughly a fourth of toluene's OH reactivity (the product of $k$ and [hydrocarbon]). The EPA Photochemical Assessment Monitoring Stations (PAMS) network includes methylcyclopentane, methylcyclohexane, 2-methylhexane, and 3-methylhexane as target hydrocarbons,[19] with 0.5 ppbC as their detection limit and 0.1 ppbC as the noise level. An accurate study of their atmospheric decay using PAMS data would be difficult because ambient levels will reach these lower limits. A more recent examination by Baker et al.[20] of nonmethane hydrocarbons in 28 U.S. cities found highly variable concentrations for toluene, indicating that levels of the $C_6-C_7$ alkanes will only be sufficiently high for an indirect [OH] urban plume measurement under polluted conditions and in certain cities. However, there are multiple cities outside of the U.S. that have reported ambient toluene concentrations[21] that indicate that the $C_6-C_7$ species will be present at ppbv levels, sufficient for an indirect [OH] measurement in the downwind plume. Measurements at Whiteface Mountain, New York[22] for all five $C_6-C_7$ alkanes in this study reach hundreds of pptv levels. These five hydrocarbons are not a part of the United Kingdom hydrocarbon network,[23] but by comparison to other hydrocarbon levels, their concentrations are expected to be significantly lower than in the United States. The other four $C_8-C_9$ alkanes in the present kinetics experiment are emitted at low levels and are not typically measured with other ambient nonmethane hydrocarbons. Their atmospheric presence would be indicative of recent hydrocarbon emissions.

## Experimental Section

Measurements were conducted using a High-Pressure Flow System (HPFS) whose configuration has been detailed previously.[24−26] Briefly, the HPFS consists of a 700 L settling chamber followed by a 10 m long, 12.36 cm internal diameter stainless steel pipe that allows the carrier gas flow to fully develop laminar flow before entering the detection zone. Nitrogen carrier gas is injected at room temperature and cooled or heated within the HPFS. In all cases, the total pressure is 8−10 torr, and the core velocity is 10−19 m $s^{-1}$. OH is generated by microwave discharge of $H_2$ in argon followed by $H + NO_2$ reaction and injection into the center of the HPFS bulk flow. Initial OH concentrations are typically below $1 \times 10^{10}$ $cm^{-3}$. The reacting laminar plume then passes through a one-meter detection region where five optical axes equally spaced by 18.4 cm detect OH by laser-induced fluorescence (LIF) perpendicular to the flow. A pitot-static probe measures the core velocity just beyond the final LIF axis. Several different concentrations of hydrocarbon are studied, all under pseudo-first-order conditions, such that the [OH] undergoes a decay of up to 2 orders of magnitude within the detection region. The rate constant is given by

$$k = -\frac{v}{\delta}\frac{\partial}{\partial n}\left(\frac{\partial \ln X_n/X_{\mathrm{ref}}}{\partial[\mathrm{XS}]}\right) \quad (1)$$

where $v$ is the core velocity (10−19 $ms^{-1}$), $\delta$ the interaxis separation (18.4 cm), $X_n$ the OH LIF signal at axis $n$, and [XS] the hydrocarbon concentration (maximum of about $10^{13}$ molecules $cm^{-3}$ for the C6−C9 species). In this paper, the third axis is chosen as the reference axis, $X_{\mathrm{ref}}$, thus accounting for variations in LIF signal independent of [OH]. A small diffusion correction (<2%) is applied to the observed decay in OH with [XS].[25] Figure 1 shows a typical plot of $\ln(X_n/X_{\mathrm{ref}})$ vs [XS] using axis 3 as the reference axis. Axes 1 and 2 are the positive slopes, and axes 4 and 5 are the negative slopes. Each rate measurement includes four different hydrocarbon concentrations for a total experimental duration of no more than 7 min.

For high-temperature measurements, the HPFS is heated slowly (with 2 kW of external resistive heaters prior to the reaction zone), so kinetics measurements are made during the several hour heating process. For low-temperature measurements, two slightly different methods of cooling were employed, with different sets of hydrocarbons for each cooling method. The first set included ethane, cyclohexane, cyclo-octane, methylcycloheptane, *n*-propylcyclohexane, and isopropylcyclohexane; the second set included ethane, cyclohexane, 2-methylhexane, 3-methylhexane, methylcyclopentane, and methylcyclohexane. For low-temperature measurements of the first set, the system is precooled to roughly 170 K by injection of liquid nitrogen for two hours. Kinetics measurements are conducted while the system warms to room temperature over the next several hours. For the second hydrocarbon set, the HPFS was cooled by liquid nitrogen passing through external copper coils ($^3/_8$ in. outside diameter), and kinetics measurements were conducted during active cooling.

The HPFS experiment depends upon the gas flow being well-defined (laminar or turbulent) and any changes in temperature in the reaction zone being small. The reaction zone is not actively heated or cooled, so the gas is slightly warmed (or cooled) by the near-ambient temperature walls of the HPFS tube during its brief residence time (a tenth of a second or less). Temperature is monitored in the core of the tube before and after the reaction zone, near the OH injection point, and near the pitot-static probe. Within the reaction zone, the gas warms by a maximum of about 3 K near 210 K, and the extent of warming is nearly linear with cooling below room temperature. Fluctuations in the average temperature in the reaction zone during a given kinetics experiment are always less than this temperature gradient. The temperature gradient is less significant at warm temperatures.

By assumption of no thermal convection and a radially uniform temperature, an axial temperature gradient will affect the observed OH decay by the consequent changes in the rate of reaction and the change in velocity down the tube

$$\frac{\partial}{\partial T}\left(\frac{\partial \ln X_n/X_{\mathrm{ref}}}{\partial[\mathrm{XS}]}\right) = \left(\frac{\partial \ln X_n/X_{\mathrm{ref}}}{\partial[\mathrm{XS}]}\right)\left(\frac{E_a}{T^2} - \frac{1}{T}\right) \quad (2)$$

where $E_a$ is a simple Arrhenius activation energy in K. The larger the temperature dependence of the rate constant, the larger is the effect of a temperature gradient. In our experiment, ethane

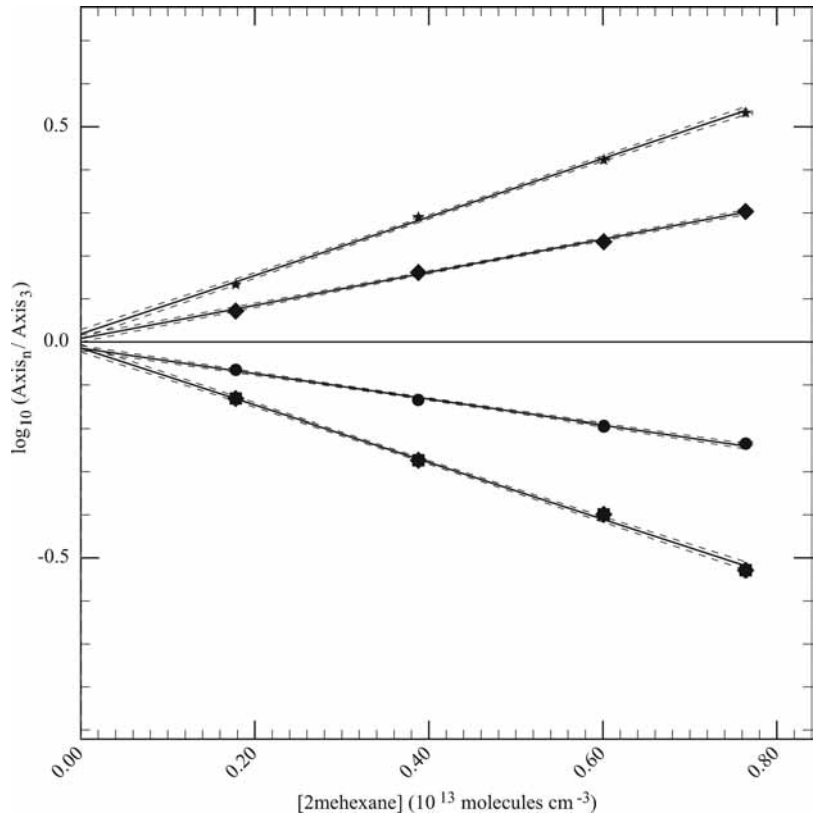


**Figure 1.** The logarithm of normalized OH fluorescence signal relative to fluorescence at the central axis (axis 3) as a function of 2-methylhexane excess reagent concentration. The linear fit lines ($\partial \ln (X_n/X_{ref})/\partial[XS]$) each provide a measurement of the rate constant (see eq 1).

has the largest temperature dependence, and at 220 K, a 3 K gradient would change the observed OH decay by about 5%. The larger alkane rate constants have significantly smaller temperature dependence, so that OH decays are typically affected by less than 2% at 220 K. Because of the very small effect, we assign all five OH detection axes the average of the initial and final experimental temperatures.

The most significant uncertainty in the rate constants is due to the measurement of the excess reagent hydrocarbons, especially for the $C_8-C_9$ cycloalkanes because of their low vapor pressures (e.g., isopropylcyclohexane, 2 torr at 288 K). In situ infrared absorption measurements of [XS] were used as the primary method, and these were complemented by measurements of relative flow via mass flow controllers and by indirect UV absorption measurements. First, gaseous mixtures of dichlorodifluoromethane (F12) and hydrocarbon were made using pressure measurements to determine the hydrocarbon mixing ratio to within 2%. The well-known UV and IR cross sections of F12 (at 189 nm and 900 $cm^{-1}$) were then used to measure the IR cross section of the hydrocarbon. At least three independent mixtures were made for each hydrocarbon to determine the reproducibility: the largest observed variability in the resulting IR cross sections was 3.5%. This approach gives a precision for [XS] of 5% or better and an accuracy of 8−9% at two $\sigma$.

Error in [XS] calibration is mostly independent of the reaction temperature and would cause all rate-constant measurements to be biased by a common factor. The second most important source of error in the rate constant is the gas velocity measurement, with an accuracy of 5−7% at two $\sigma$. The velocity error may be sensitive to temperature, with a systematic error of a few percent over the full temperature range.

In the present work, room-temperature reference IR cross sections were used to determine [XS] over the full temperature range studied: 221−385 K. Separate analyses for [XS] using relative flow rates and UV absorption of F12 were made to verify that the room-temperature IR spectrum remained suitable for calibration. These three methods gave results that agreed to within 2% for all compounds except for ethane, which gave a 10% systematic deviation in its IR analysis at both temperature extremes when compared with the flow and F12 UV analyses. The ethane IR band is broader than that of the other compounds, so its spectrum should be most sensitive to changes in temperature. For the first hydrocarbon set (ethane, cyclohexane, cyclo-octane, methylcycloheptane, *n*-propylcyclohexane, and isopropylcyclohexane), relative flow calibrated at room temperature by IR absorption was chosen as the most accurate method for measuring [XS]. During the second set of experiments (ethane, cyclohexane, 2-methylhexane, 3-methylhexane, methylcyclopentane, and methylcyclohexane), the three independent methods for measuring [XS] showed disagreement at low temperatures, as shown in Figure 2 for methylcyclohexane. The relative flow and UV absorption measurements both indicated higher concentrations (and consequently lower rates of reaction) than the direct IR measurement. We interpret this discrepancy to indicate some deposition (up to 15%) of our excess hydrocarbon reagent onto the upstream HPFS walls in direct contact with the external liquid nitrogen cooling tubes. Because this deposition occurs along more than 8 m of tubing, it is too small to create a significant radial gradient in [XS]. For the second set of hydrocarbons, we chose direct IR absorption as the most accurate method for measuring [XS] and excluded concurrent ethane measurements from our presently reported values because of its sensitivity to temperature in the IR.

During the first set of hydrocarbon measurements, there was also evidence of wall deposition at the lowest temperatures obtained, around 180 K. Upon addition of cycloalkane reagent,

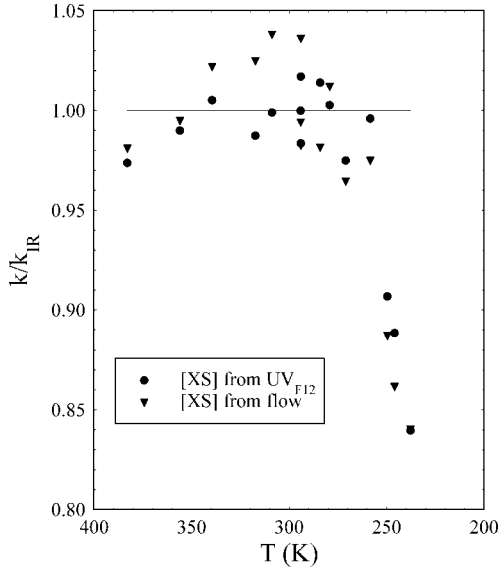


**Figure 2.** Rate constant results while measuring the concentration of methylcyclohexane excess reagent ([XS]) with relative flows and UV absorption of F12 are compared to results using direct IR detection of [XS] as a function of temperature. Low-temperature results indicate that the hydrocarbon excess reagent was adsorbing to the flow tube wall upstream of the reaction zone. For all other temperature regimes, the three methods of measuring [XS] agree to better than ±4%.

the OH fluorescence signal required tens of seconds to equilibrate, most likely because of loss to the wall of alkane. Only isopropylcyclohexane exhibited this behavior above 220 K, and its rate constants are reported for temperatures of 260 K and greater, where this delay in equilibration is not observed. Because the in situ measurement of hydrocarbon is directly between the first and second detection axes and the walls of the detection zone are not actively cooled, the measurement of [XS] is not affected by the upstream wall deposition.

A set of six criteria was applied to the measurements prior to their acceptance into the final data set. (1) On each day of measurements, ethane's rate constant agrees within 10% with our laboratory's previous measurements for this reference compound. (2) Each kinetics measurement includes depletion of OH over 2 orders of magnitude without evidence of OH regeneration by secondary chemistry. (3) The temperature gradient in the reaction zone is ≤3 K. (4) The three independent measurements of [XS] are in good agreement at room temperature. (5) The four decay rates measured between pairs of axes exhibit less than 10% variability. (6) Forcing a zero intercept into the plot of $\ln(X_n/X_{ref})$ vs [XS] affects the measured slope by less than 10% (see eq 1).

In general, we observed a slightly higher slope for $\ln(X_n/X_{ref})$ vs [XS] when a zero intercept is included (5 ± 2% for ethane; 4 ± 2% cyclohexane; 1 ± 1% methylcyclopentane; 2 ± 1% methylcyclohexane; 3 ± 2% 3-methylhexane; 5 ± 2% 2-methylhexane). This effect may be attributed to miscalibration of [XS] or to a very small amount of OH regeneration via secondary chemistry. The results reported herein include the zero intercept. Finally, a comparison of assigning axis 1 vs axis 3 as reference axes demonstrated that the analysis of $\partial \ln(X_n/X_{ref})/\partial[XS]$ was insensitive to the chosen reference axis. Figure 1 shows a typical plot of $\ln(X_n/X_{ref})$ vs [XS] using axis 3 as the reference axis and excluding the zero intercept. Inclusion of the zero intercept in this plot would slightly increase the magnitude ofrted in Table 1 the measured slopes.

Alkanes were obtained from the following sources: ethane, union carbide; 99.99% cyclohexane, EM Science; 99+% cyclo-

**TABLE 1: Averaged Rate Constant Measurements ($10^{-13}$ cm$^3$ s$^{-1}$) Adjusted to Reference Temperatures**[a]

| *T* (K) | ethane | cyclohexane | cyclo-octane | 2-methyl- hexane | 3-methyl- hexane | methylcyclopentane | methylcyclo hexane | methylcycloheptane | propylcyclohexane | isopropylcyclohexane |
|---|---|---|---|---|---|---|---|---|---|---|
| 221 | 0.67 ± 0.02 | 46.0 ± 2.3 | | | | | | | | |
| 230 | 0.77 ± 0.02 | 50.5 ± 1.2 | | 61.5 ± 2.2 | 52.0 ± 1.8 | 69.5 ± 0.7 | 88.1 ± 3.9 | 122.7 ± 5.2 | 116.7 ± 7.6 | |
| 237 | 0.87 ± 0.02 | 53.8 ± 0.8 | 119.4 ± 4.2 | 60.8 ± 2.2 | 58.7 ± 1.3 | 66.7 ± 1.1 | 86.0 ± 2.9 | | 113.5 ± 5.1 | |
| 245 | 1.03 ± 0.02 | 54.9 ± 0.7 | | 58.5 ± 1.0 | 61.6 ± 1.2 | 70.0 ± 2.6 | 86.5 ± 1.3 | 128.2 ± 5.2 | 114.3 ± 4.6 | |
| 260 | 1.38 ± 0.02 | 59.5 ± 0.5 | 135.2 ± 2.6 | 60.4 ± 5.1 | 61.9 ± 2.1 | 70.8 ± 3.5 | 89.2 ± 4.1 | 125.7 ± 5.2 | 119.5 ± 3.5 | 137.9 ± 3.2 |
| 275 | 1.80 ± 0.02 | 65.6 ± 0.5 | 136.4 ± 2.8 | 61.6 ± 3.1 | 64.0 ± 1.3 | 73.5 ± 0.9 | 92.8 ± 1.7 | 139.1 ± 5.2 | 124.9 ± 2.9 | 140.3 ± 2.5 |
| 290 | 2.39 ± 0.02 | 71.9 ± 0.4 | 143.4 ± 2.6 | 66.9 ± 1.0 | 63.0 ± 0.7 | 76.6 ± 0.6 | 92.9 ± 1.3 | 150.6 ± 5.2 | 133.2 ± 2.9 | 143.9 ± 2.5 |
| 305 | 2.91 ± 0.07 | 76.4 ± 0.5 | 144.3 ± 2.6 | 68.2 ± 2.0 | 71.1 ± 2.9 | 74.7 ± 1.7 | 95.9 ± 1.3 | | | 136.0 ± 2.5 |
| 320 | 3.56 ± 0.04 | 81.2 ± 0.8 | 147.0 ± 3.1 | 69.9 ± 1.6 | 67.4 ± 1.0 | 80.8 ± 1.5 | 96.2 ± 2.1 | 153.9 ± 5.2 | 139.3 ± 2.9 | 151.3 ± 2.9 |
| 335 | 4.06 ± 0.07 | 84.9 ± 0.6 | 155.1 ± 2.6 | 75.1 ± 1.9 | 72.5 ± 2.2 | 87.0 ± 0.6 | 105.6 ± 1.3 | 156.9 ± 9.0 | 143.0 ± 5.5 | 139.8 ± 2.5 |
| 350 | 4.57 ± 0.02 | 86.4 ± 0.8 | 160.1 ± 2.6 | 72.7 ± 3.2 | 70.6 ± 0.7 | 82.4 ± 2.2 | 101.2 ± 3.3 | 152.8 ± 5.2 | 144.4 ± 6.1 | 134.8 ± 5.3 |
| 360 | 4.93 ± 0.09 | 88.0 ± 0.7 | 156.2 ± 4.8 | 74.3 ± 2.7 | 75.3 ± 1.7 | 88.7 ± 3.5 | 109.2 ± 1.3 | | 141.3 ± 4.6 | 144.1 ± 4.9 |
| 370 | 5.86 ± 0.31 | 91.8 ± 1.5 | | 78.1 ± 2.9 | | 83.2 ± 1.7 | 102.1 ± 3.4 | | 138.9 ± 4.6 | |
| 379 | 6.16 ± 0.04 | 98.3 ± 1.4 | 163.5 ± 3.3 | 78.1 ± 3.3 | 81.0 ± 1.9 | | 103.7 ± 1.3 | | 152.7 ± 4.4 | 145.0 ± 4.3 |
| 385 | | 96.4 ± 3.5 | | 80.5 ± 1.1 | 77.6 ± 0.7 | | | | | |
| no. data | 78 | 168 | 29 | 45 | 35 | 43 | 47 | 22 | 20 | 41 |

[a] Reported uncertainties reflect experimental precision. Overall accuracy is 10% at room temperature and 12% at the two temperature limits (two $\sigma$).

**TABLE 2: Modified Arrhenius Fit Results[a]**

| alkane | $B$ ($10^{-9}$Kcm$^3$s$^{-1}$) | $E_a$ (K) | $k_{fit}(298)$ ($10^{-12}$ cm$^3$ s$^{-1}$) | $k_{fit}(290)$ ($10^{-12}$ cm$^3$ s$^{-1}$) | $k_{fit}(260)$ ($10^{-12}$ cm$^3$ s$^{-1}$) |
|---|---|---|---|---|---|
| cyclohexane (this work) | $3.24 \pm 0.14$ | $332 \pm 12$ | 7.13 | 6.88 | 5.97 |
| cyclohexane (fit to all) | $3.09 \pm 0.12$ | $326 \pm 12$ | 6.96 | 6.72 | 5.85 |
| cyclo-octane | $3.47 \pm 0.30$ | $149 \pm 26$ | 14.1 | 13.8 | 12.9 |
| 2-methylhexane | $1.45 \pm 0.08$ | $110 \pm 15$ | 6.72 | 6.62 | 6.28 |
| 3-methylhexane | $1.50 \pm 0.08$ | $128 \pm 16$ | 6.54 | 6.44 | 6.06 |
| methylcyclopentane | $1.65 \pm 0.07$ | $109 \pm 13$ | 7.65 | 7.54 | 7.15 |
| methylcyclohexane | $1.86 \pm 0.09$ | $83 \pm 14$ | 9.43 | 9.32 | 8.93 |
| methylcycloheptane | $3.45 \pm 0.45$ | $142 \pm 36$ | 14.4 | 14.1 | 13.2 |
| propylcyclohexane | $2.83 \pm 0.14$ | $112 \pm 15$ | 13.0 | 12.8 | 12.2 |
| isopropylcyclohexane | $1.79 \pm 0.11$ | $-44 \pm 34$ | 13.9 | 13.9 | 14.0 |

[a] Two bends at 280 cm$^{-1}$ and one bend at 500 cm$^{-1}$ are treated explicitly (eq 3). Uncertainties are one $\sigma$ result from linear regression fits and are likely underestimated (see text).

octane, 99% isopropylcyclohexane, 99% 2-methylhexane, 99% 3-methylhexane, 99% methylcyclohexane and 99% propylcyclohexane, Aldrich Chemical Co.; 98% methylcyclopentane, TCI America; 99% methylcycloheptane, Wiley Organics. Three freeze−pump−thaw cycles removed more volatile contaminants.

## Results

The data set of over 500 individual rate-constant measurements are grouped by temperature and are repo. Each individual measurement is adjusted to a reference temperature using a modified Arrhenius fit to the entire data set: $k(T_{ref}) = k_{exp}(T) \times (k_{fit}(T_{ref})/k_{fit}(T))$. Multiple measurements at the same reference temperature are then averaged and their standard deviation, which reflects experimental precision, is also reported in Table 1. The overall accuracy of the measurements is 10% at room temperature and reaches 12% at the temperature limits (at two $\sigma$). Ethane kinetics data were used for quality assurance, and measurements were in excellent agreement with previous studies in our laboratory.[26] Small differences at the temperature extremes are attributed to the calibration of ethane using a room-temperature IR cross section in the previous study (see experimental section).

The full raw data set for each reaction is fit to the following modified Arrhenius equation[27]

$$k(T) = \frac{Be^{-E_a/T}}{T(1 - e^{-1.44\nu_1/T})^2(1 - e^{-1.44\nu_2/T})} \qquad (3)$$

that is based upon transition state theory (ignoring tunneling). $B$ is the pre-exponential factor, $E_a$ is the activation barrier in Kelvin, $T$ is temperature, and $\nu_1$ and $\nu_2$ are bending frequencies, set to 280 and 500 cm$^{-1}$ for C−H−O and H−O−H bends, respectively. This expression more fully accounts for the temperature dependence of the rate constant and is preferred over the simple Arrhenius form ($Be^{-E_a/T}$) or the too highly curved $T^2$ form ($BT^2e^{-E_a/T}$), especially for temperatures significantly below 270 K. Furthermore, the $T^2$ form produces an effective barrier that is not obviously related to a transition state energy. The vibrational frequencies used in eq 3 are derived from low level ab initio calculations (UHF/6-31G**) and are assumed to be the same for all alkanes. In actuality, the vibrational frequencies of different alkanes are almost certainly correlated with barrier heights,[28] but our experimental error is larger than the effect of subtle variations in these bending frequencies. Thus our experimental results cannot justifiably be used to further constrain $\nu_1$ and $\nu_2$.

The fit results are summarized in Table 2 together with one $\sigma$ uncertainties. Figure 3 presents line plots of the fits covering the temperature range for each data set. Residuals of the data relative to the fits are presented in Figures 4 and 5. Previous cycloheptane results from our laboratory[25] are included in Figure 3 for comparison. Of the compounds studied, only cyclohexane has previously reported temperature-dependent data outside of our research group. Our group has studied both cyclohexane and cyclo-octane from 300−390 K,[27] and the results are consistent, with slightly more scatter in the earlier data. Both data sets are included in the cyclo-octane fit.

Cyclohexane provides the only opportunity for extensive comparison with other measurements. The results are presented in Figure 5. The upper portion of Figure 5 provides a standard Arrhenius plot of ln($k$) vs 1/$T$, and the lower portion shows the residuals of the data relative to the fit for all 52 data points. Two fits were conducted for cyclohexane. The first fit encompassed only the present data set and was used for grouping the data to reference temperatures (in Table 1). The second fit encompassed 17 separate studies, totaling 25 relative and 27 direct rate measurements, including 22 data points from three HPFS studies in our laboratory. The latter fit is displayed in Figure 5. For previous relative rate constant measurements, we use a best fit to the modified Arrhenius equation (eq 3) for the reference reaction using reported measurements from multiple laboratories. The significant discrepancy at low temperature between the Wilson et al.[30] data points and their corresponding fit to those data (also provided in Figure 5) results primarily from their use of the simple Arrhenius rate form for both cyclohexane and for the reference compound, *n*-butane. Our best fit to *n*-butane data from multiple laboratories[44] is also a few percent above the data set of DeMore and Bays[38] used in the simple Arrhenius fit in Wilson et al.[30] Measurements from four additional studies (Greiner,[39] Edney et al.,[34] Nielsen et al.,[40] and Bourmada et al.[42]) are shown in Figure 5 but were excluded from the fit analysis.

## Comparison to Literature

For the cyclohexane data presented in Figure 5, we compare each experiment to the final fit with two measures: first the average percentage deviation from the fit, and second the standard deviation of the percent deviation from the fit (when there are two or more data points). The first measure indicates agreement with the fit while the second can indicate large variations in the data set or a systematic disagreement with temperature. The results for the cyclohexane fit are as follows: Atkinson et al.[31] 1.03, Tuazon et al.[32] 1.01, Atkinson et al.[33] 1.01, Edney et al.[34] 0.86, Atkinson and Aschmann[35] 1.00, Sommerlade[36] 1.04, Kramp and Paulson[37] 1.04, DeMore and Bayes[38] 1.03 ± 0.01 (butane), 0.96 ± 0.01 (pentane), 0.96 ± 0.005 (propane), Wilson et al.[30] 0.95 ± 0.02, Greiner[39] 1.03 ±

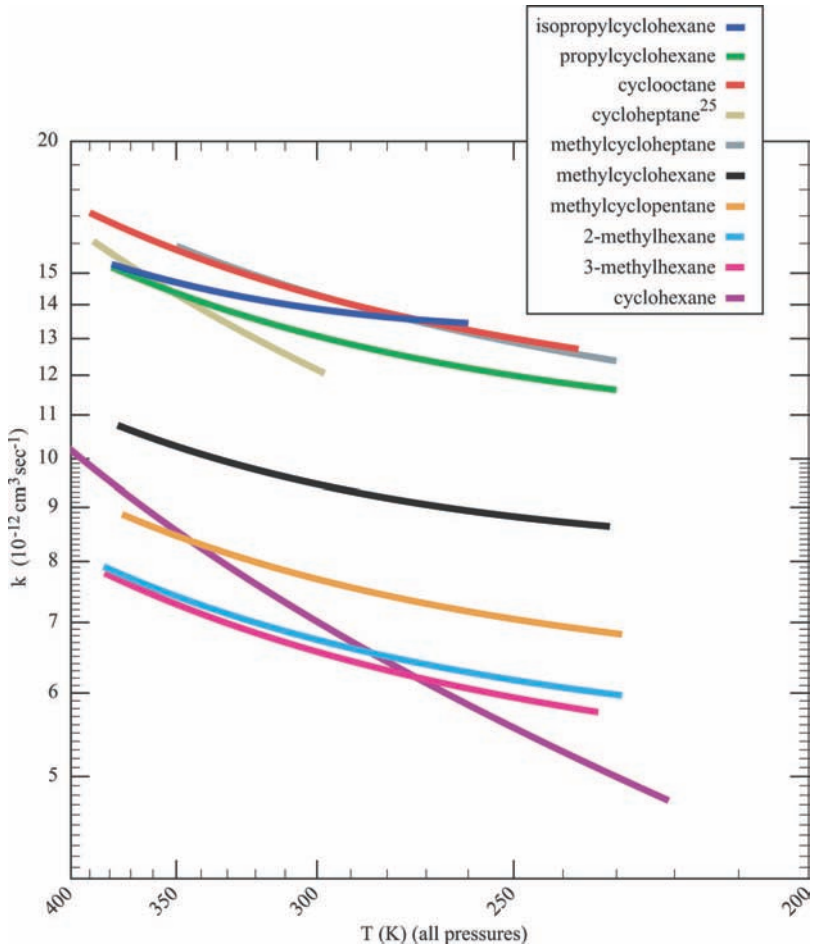


**Figure 3.** Fit results presented in Table 2 are plotted over the experimental temperature range for all nine compounds studied. Cycloheptane data from Donahue et al.[27] are included for comparison. Note the dramatic difference in the temperature dependence for isopropylcyclohexane, with two tertiary hydrogens. Cyclohexane and cyclo-octane have significantly different barriers ($E_a$).

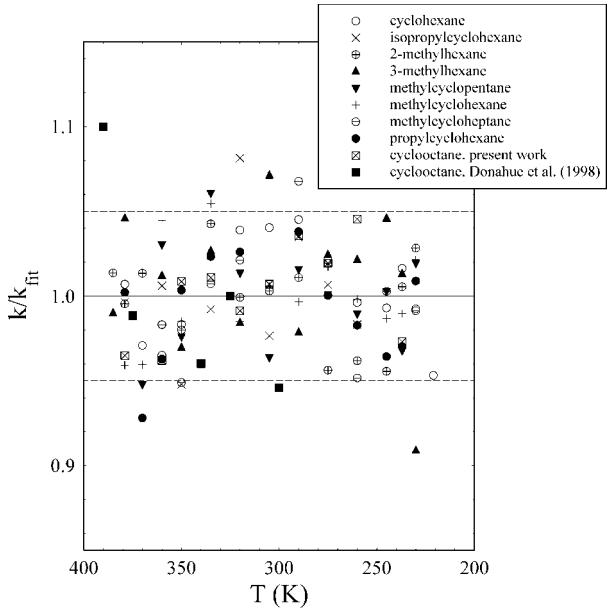


**Figure 4.** Residuals of binned data presented in Table 1 relative to fit results. The residuals rarely exceed 5% and are fairly random about the fit.

0.13, Nielsen et al.[40] 0.76, Droege and Tully[41] 1.01 ± 0.04, Bourmada et al.[42] 1.25, Saunders et al.[43] 0.96, Donahue et al.[25] 1.08, Donahue et al.[27] 1.03 ± 0.06, present work 1.03 ± 0.03. The HPFS result is consistently 7−8% higher than the fit at room temperature. Other results, both absolute and relative (Saunders et al.[43] and DeMore and Bayes[38]) are 4% lower than the fit result at room temperature, giving a 12% total spread at room temperature, excluding 3 outliers.

The cyclohexane data shown in Figure 5 possess several characteristics that are typical of many alkane + OH kinetic data sets.[27,28,38] Nearly all of the data since 1987 fall within ±10% of the fit. The low-temperature data, below 270 K, do not exhibit the curvature described by a $T^2$ functional form $T^2e^{-E_a/T}$, as assumed by Atkinson,[29] nor the simple Arrhenius form $Be^{-E_a/T}$, as assumed by Wilson et al.[30] The experimentally derived barrier to reaction ($E_a$) varies across studies by more than the uncertainty obtained by a linear regression fit to all of the data (consider Greiner,[39] Droege and Tully,[41] DeMore and Bayes,[38] Wilson et al.,[30]Donahue et al.,[27] and the present work). Interexperiment variation for $E_a$ of cyclohexane is typically 100 K (with smaller temperature ranges than the present work). These differences reflect systematic errors that correlate with temperature. Considering all data, the regression fit uncertainty is 24 K at two $\sigma$. The present experiment significantly increases the temperature range of absolute rate constant measurements for this reaction, and the temperature dependence is in excellent agreement with the recent relative measurements over a similar temperature range by Wilson et al.[30] Given the large temperature range of the data and the availability now of several independent temperature-dependent measurements, the $E_a$ for cyclohexane is constrained to ±40 K (two $\sigma$).

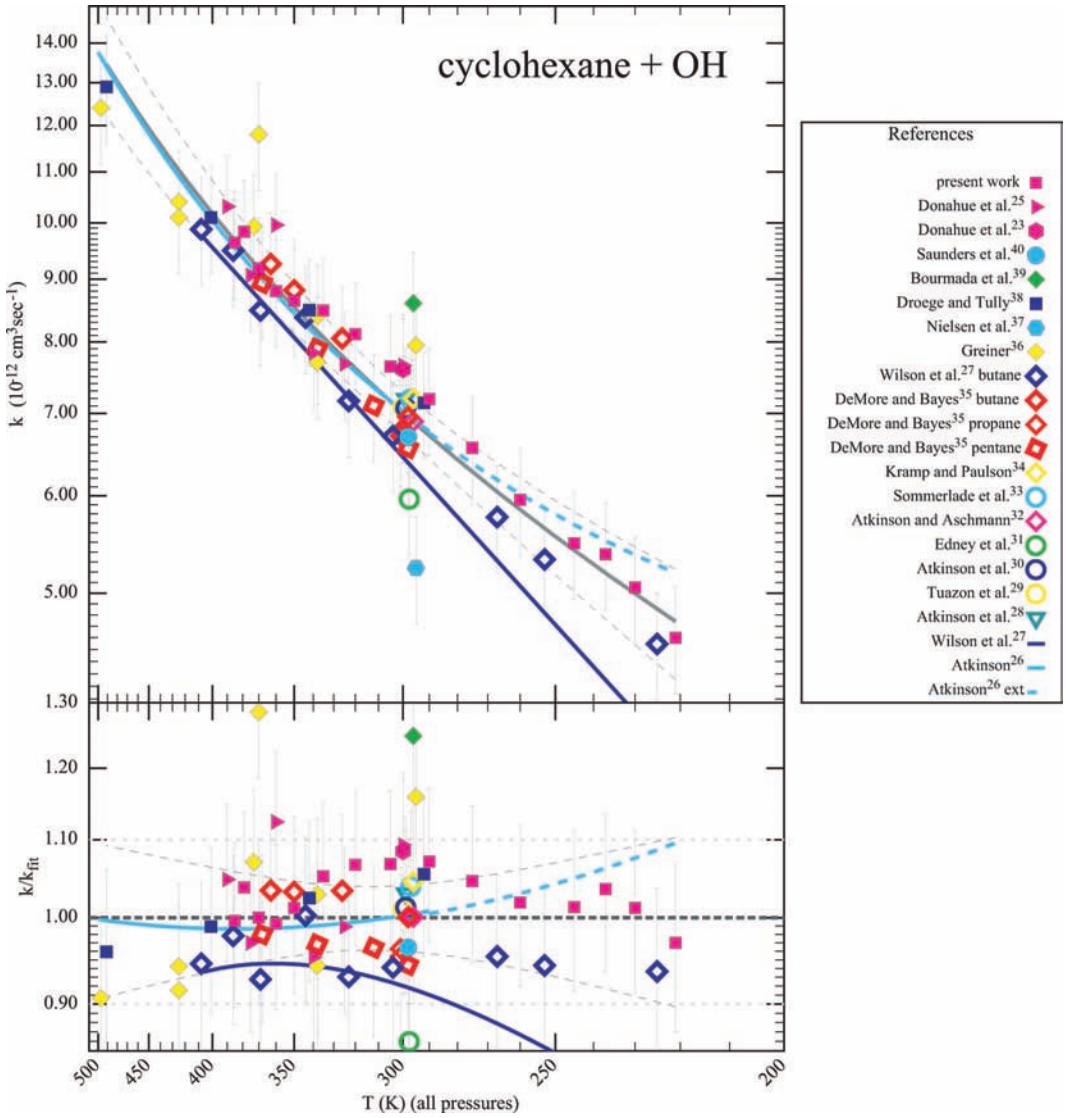


**Figure 5.** Cyclohexane rate constant data as a function of temperature. The bottom half of the figure shows an expansion about the final fit to the results of multiple studies. While recent warm and cold data generally agree within about 5% of the fit, there is a wider variation in the room temperature data set. No low temperature data was available to constrain the Atkinson fit.[29]

Cyclo-octane has been measured directly by Behnke,[45] giving a result 3% lower than the present fit at 300 K. Our laboratory's previous study of cyclo-octane[27] agrees with the present work within 1% with a standard deviation of 6% for the residuals about the fit. Methylcyclohexane was measured by Kramp and Paulson[37] by a relative method against several compounds, giving a result that agrees with our fit result to better than 1%. Atkinson et al.[46] measured its rate constant relative to *n*-butane and obtained a result 6% higher than our fit. Methylcyclopentane was measured relative to cyclopentane at room temperature by Anderson et al.[47] with a result that is 12% higher than the present work.

## Discussion

Five of the nine compounds in this study have no previous data available for intercomparison. This data set of accurate rate coefficients of reaction makes accessible a new suite of compounds for laboratory calibration or field measurement of [OH]. Before exploring homologous sequences, we must estimate the uncertainty in experimentally measured activation barriers ($E_a$). If our data possesses a 10% systematic error that correlates with temperature (+10% at low $T$ and −10% at high $T$, for example), then the $E_a$ will change by 100 K for $C_6/C_7$ species and 120 K for $C_8/C_9$ species. While this limit of uncertainty is overly conservative, previous studies[27,29,38] do indicate a larger uncertainty in $E_a$ than obtained from regression uncertainty alone (because regression only considers experimental precision and not overall accuracy). Until additional data is reported for intercomparison, a reasonable uncertainty in $E_a$ for these new compounds is ±75 K for $C_6/C_7$ species and ±90 K for $C_8/C_9$ species (two $\sigma$). This magnitude of uncertainty indicates that for these species the uncertainty in $E_a$ is very large in comparison to its magnitude. This makes comparison with subtle theoretical considerations difficult.

Table 2 and Figure 3 reveal several patterns concerning the set of alkanes. As expected, 2- and 3-methylhexane have the same reactivity. The barrier for the methylcycloalkane series is unchanged in going from methylcyclopentane up to methylcycloheptane, considering the uncertainty in $E_a$. Indeed, all species with a lone tertiary hydrogen have barriers close to 115 K. Isopropylcyclohexane, with two tertiary hydrogens, has a markedly lower barrier, −44 K. At low temperatures, the effects of vibrational activation at the transition state are minimized, while the effects directly tied to the barrier (i.e., the height itself

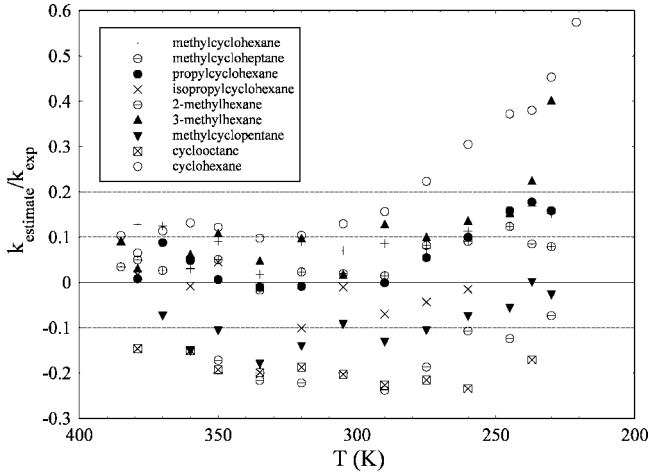


**Figure 6.** Ratio of estimated rate coefficient of reaction using Kwok and Atkinson empirical structure reactivity method[50] to experimental result.

and tunneling) are maximized.[45] Consequently, the low-temperature results reported here emphasize those barrier effects.

The surprising result in Table 2 is that cyclohexane exhibits a significantly higher barrier than cyclo-octane: 326 vs 149 K. Previous studies had indicated that the secondary hydrogen barrier in the homologous sequence of cycloalkanes reaches a fixed value for $\geq C_5$ rings.[27,30,48] Transition state theory and theoretical work within our group[49] indicate that there should not be a significant difference in these barriers to first order. The low-temperature measurements of the present experiment strongly influence the shift in these barriers from previously reported nearly equal values.[27] The difference in cyclohexane and cyclo-octane barriers is independent of the type of fit that is chosen: a simple Arrhenius fit ($Be^{-E_a/T}$) gives a slightly larger barrier (by about 50 K) with the same barrier difference. For comparison, Figure 3 shows the line fit to cycloheptane from Donahue et al.[27] Its reactivity is close to that of cyclo-octane, but its barrier is more similar to cyclohexane. However, with a smaller temperature range, there is a larger uncertainty in its barrier.

Room-temperature experimental rate constants tend to be higher, on average 2.6% higher, than the fit result to all data indicate. The rate constants at the two temperature extremes tend to fall below the fit curve. This pattern indicates that the modified Arrhenius fit is somewhat too curved for the compounds in this study. The frequencies used for $\nu_1$ and $\nu_2$ in eq 2 are correlated with the barrier height, and average values for the set of OH + alkane abstraction reactions have been used in the current fits.[27] The deviation of the data from the fit curve (see Figure 4) is only a few percent and is much smaller than other sources of error in the data.

Kwok and Atkinson[50] have developed an empirically based estimation for the hydrogen abstraction reactions of OH with hydrocarbons, and we have compared their estimates to the current experimental results as summarized in Figure 6. At room temperature, $C_7$ and $C_8$ ring estimates are too low and show the largest difference from experimental measurement. Their estimates are within 25% of the experimental results, and all other room temperature estimates are within 15% of experimental results. For all compounds, estimates rise faster than the experimental measurements at temperatures below 260 K. At 221 K, cyclohexane has the largest difference, with empirical estimation 57% higher than the experimental value. The Kwok and Atkinson estimation scheme uses a $T^2$ form for the rate coefficient, which is too curved to describe the temperature dependence at the lowest temperatures.

## Conclusions

We report over 500 independent rate measurements for nine $C_6-C_9$ alkanes. Five of these rates are reported for the first time. Our data for cyclohexane, methylcyclopentane, methylcyclohexane, 2-methylhexane, and 3-methylhexane can contribute to efforts to use atmospheric hydrocarbon decay as an indirect measure of ambient [OH]. The larger temperature range of rate constants for cyclohexane and cyclo-octane indicate that these two species have significantly different reaction barriers. This surprising result could be further explored by future low-temperature kinetics studies of cyclopentane and cycloheptane. Independent measurements for cyclo-octane's temperature dependence would also improve the confidence in this result.

**Acknowledgment.** This work was supported by U.S. Environmental Protection Agency STAR Grant (R825258010) to SUNY at Albany and Harvard University and National Science Foundation Grant (9977992) to Harvard University.

## References and Notes

(1) Demerjian, K. L.; Kerr, J. A.; Calvert, J. G. *Adv. Environ. Sci. Technol.* **1974**, *4*, 1–262.
(2) Wu, C. H.; Japar, S. M.; Niki, H. *J. Environ. Sci. Health A* **1976**, *A11*, 191.
(3) Hard, T. M.; George, L. A.; O'Brien, R. J. *Environ. Sci. Technol.* **2002**, *36* (8), 1783–1790.
(4) Calvert, J. G. *Environ. Sci. Technol.* **1976**, *10*, 256.
(5) Roberts, J. M.; Fehsenfeld, F. C.; Liu, S. C.; Bollinger, M. J.; Hahn, C.; Albritton, D. L.; Sievers, R. E. *Atmos. Environ.* **1984**, *18*, 2421.
(6) Blake, N. J.; Penkett, S. A.; Clemitshaw, K. C.; Anwyl, P.; Lightman, P.; Marsh, A. R. W.; Butcher, G. *J. Geophys. Res.* **1993**, *98*, 2851.
(7) Hopkins, J. R.; Barnett, C. J.; Lewis, A. C.; Seakins, P. W. *J. Environ. Monit.* **2003**, *5*, 14–20.
(8) McKeen, S. A.; Trainer, M.; Hsie, E. Y.; Tallamraju, R. K.; Liu, S. C. *J. Geophys. Res.* **1990**, *95*, 7493.
(9) Ehhalt, D. H.; Rohrer, F.; Wahner, A.; Prather, M. J.; Blake, D. R. *J. Geophys. Res.* **1998**, *103*, 18981–18997.
(10) Jobson, B. T.; Parrish, D. D.; Goldan, P.; Kuster, W.; Fehsenfeld, F. C.; Blake, D. R.; Blake, N. J.; Niki, H. *J. Geophys. Res.* **1998**, *103*, 13557–13567.
(11) Jobson, B. T.; McKeen, S. A.; Parrish, D. D.; Fehsenfeld, F. C.; Blake, D. R.; Goldstein, A. H.; Schauffler, S. M.; Elkins, J. W. *J. Geophys. Res.* **1999**, *104*, 16091–16113.
(12) McKeen, S. A.; Liu, S. C.; Hsie, E. Y. *J. Geophys. Res.* **1996**, *101*, 2087–2109.
(13) Kramp, F.; Volz-Thomas, A. *J. Atmos. Chem.* **1997**, *28*, 263–282.
(14) Parrish, D.; Trainer, M.; Young, V.; Goldan, P.; Kuster, W.; Jobson, B.; Fehsenfeld, F.; Lonneman, W.; Zika, R.; Farmer, C.; Riemer, D.; Rodgers, M. *J. Geophys. Res.* **1998**, *103*, 22339–22359.
(15) Dillon, M. B.; Lamanna, M. S.; Schade, G. W.; Goldstein, A. H.; Cohen, R. C. *J. Geophys. Res.* **2002**, *107*, 4045.
(16) Price, H. U.; Jaffe, D. A.; Cooper, O. R.; Doskey, P. V. *J.Geophys. Res* **2004**, *109*, D23S13.
(17) Arnold, S. R.; Methven, J.; Evans, M. J.; Chipperfield, M. P.; Lewis, A. C.; Hopkins, J. R.; McQuaid, J. B.; Watson, N.; Purvis, R. M.; Lee, J. D.; Atlas, E. L.; Blake, D. R.; Rappengluck, B. *J. Geophys. Res* **2007**, *112*, D10S40.
(18) Seila, R. L.; Lonneman, W. A.; Meeks, S. A. "Project Summary: Determination of C2 to C12 Ambient Air Hydrocarbons in 39 U.S. Cities from 1984 through 1986," E.P.A., 1989.
(19) Demerjian, K. L. *Atmos. Environ.* **2000**, *34*, 1861–1884.
(20) Baker, A.; Beyersdorf, A.; Doezema, L.; Katzenstein, A.; Meinardi, S.; Simpson, I.; Blake, D.; Rowland, F. *Atmos. Environ.* **2008**, *42*, 170–182.
(21) Guo, H.; So, K.; Simpson, I.; Barletta, B.; Meinardi, S.; Blake, D. *Atmos. Environ.* **2007**, *41*, 1456–1472.
(22) Gong, Q.; Demerjian, K. L. *J. Geophys. Res.* **1997**, *102*, 28059–28069.
(23) Derwent, R. G.; Davies, T. J.; Delaney, M.; Dollard, G. J.; Field, R. A.; Dumitrean, P.; Nason, P. D.; Jones, B. M. R.; Pepler, S. A. *Atmos. Environ.* **2000**, *34*, 297–312.

(24) Abbatt, J. P. D.; Demerjian, K. L.; Anderson, J. G. *J. Phys. Chem.* **1990**, *94*, 4566–75.
(25) Donahue, N. M.; Clarke, J. S.; Demerjian, K. L.; Anderson, J. G. *J. Phys. Chem.* **1996**, *100*, 5821–38.
(26) Clarke, J. S.; Kroll, J. H.; Donahue, N. M.; Anderson, J. G. *J. Phys. Chem. A* **1998**, *102*, 9847–9857.
(27) Donahue, N. M.; Anderson, J. G.; Demerjian, K. L. *J. Phys. Chem. A* **1998**, *102*, 3121–3126.
(28) Donahue, N. M.; Clarke, J. S.; Anderson, J. G. *J. Phys. Chem. A* **1998**, *102*, 3923–3933.
(29) Atkinson, R. *Atmos. Chem. Phys.* **2003**, *3*, 2233–2307.
(30) Wilson, E.; Hamilton, W.; Kennington, H.; Evans, B.; Scott, N.; DeMore, W. *J. Phys. Chem. A* **2006**, *110*, 3593–3604.
(31) Atkinson, R. A.; Aschmann, S. M.; Winer, A. M.; Pitts, J. N., Jr. *Int. J. Chem. Kinet.* **1982**, *14*, 507–516.
(32) Tuazon, E. C.; Carter, W. P. L.; Atkinson, R.; Pitts, J. N., Jr. *Int. J. Chem. Kinet.* **1983**, *15*, 619–629.
(33) Atkinson, R.; Aschmann, S. M.; Pitts, J. N., Jr. *Int. J. Chem. Kinet.* **1983**, *15*, 75–81.
(34) Edney, E. O.; Kleindienst, T. E.; Corse, E. W. *Int. J. Chem. Kinet.* **1986**, *18*, 1355–1371.
(35) Atkinson, R.; Aschmann, S. M. *Int. J. Chem. Kinet.* **1992**, *24*, 983–989.
(36) Sommerlade, R.; Parlar, H.; Wrobel, D.; Kochs, P. *Environ. Sci. Technol.* **1993**, *27*, 2435–2440.
(37) Kramp, F.; Paulson, S. E. *J. Phys. Chem. A* **1998**, *102*, 2685–2690.
(38) DeMore, W. B.; Bayes, K. D. *J. Phys. Chem. A* **1999**, *103*, 2649–2654.
(39) Greiner, N. R. *J. Chem. Phys.* **1970**, *53*, 1070–1076.
(40) Nielsen, O. J.; Munk, J.; Pagsberg, P.; Sillesen, A. *Chem. Phys. Lett.* **1986**, *128*, 168–171.
(41) Droege, A. T.; Tully, F. P. *J. Phys. Chem.* **1987**, *91*, 1222–1225.
(42) Bourmada, N.; Lafage, C.; Devolder, P. *Chem. Phys. Lett.* **1987**, *136*, 209–214.
(43) Saunders, S. M.; Baulch, D. L.; Cooke, K. M.; Pilling, M. J.; Smurthwaite, P. I. *Int. J. Chem. Kinet.* **1994**, *26*, 113–130.
(44) Donahue, N. M.; Clarke, J. S. *Int. J. Chem. Kinet.* **2004**, *36*, 259–272.
(45) Behnke, W.; Hollander, W.; Koch, W.; Nolting, F.; Zetzsch, C. *Atmos. Environ.* **1988**, *22*, 1113–1120.
(46) Atkinson, R.; Carter, W. P. L.; Aschmann, S. M.; Winer, A. M.; Pitts, J. N. *Int. J. Chem. Kinet.* **1984**, *16*, 469–481.
(47) Anderson, R. S.; Huang, L.; Iannone, R.; Thompson, A. E.; Rudolph, J. *J. Phys. Chem. A* **2004**, *108*, 11537–11544.
(48) Sage, A. M.; Donahue, N. M. *J. Photochem. Photobiol.* **2005**, *176*, 238–249.
(49) Donahue, N. M. *J. Phys. Chem. A* **2001**, *105*, 1489–1497.
(50) Kwok, E. S. C.; Atkinson, R. *Atmos. Environ.* **1995**, *29*, 1685–1695.

JP810412M